JTTEE5 20:3–11
DOI: 10.1007/s11666-010-9577-x
1059-9630/$19.00 © ASM International

Improving Powder Injection in Plasma Spraying by Optical Diagnostics of the Plasma and Particle Characterization

Georg Mauer, Robert Vaßen, Detlev Stöver, Stefan Kirner, José-Luis Marqués, Stephan Zimmermann, Günter Forster, and Jochen Schein

(Submitted April 26, 2010; in revised form October 4, 2010)

Powder injection parameters such as gas flow, injection angle, and injector position strongly influence the particle beam and thus coating properties. The interaction of the injection conditions on particle properties based on DPV-2000 measurements using the single-cathode F4 torch is presented. Furthermore, the investigation of the plasma plume by emission computer tomography is described when operating the three-cathode TriplexPro™ torch. By this imaging technology, the three-dimensional shape of the radiating plasma jet is reproduced based on images achieved from three CCD cameras rotating around the plume axis. It is shown how the formation of the plasma jet changes with plasma parameters and how this knowledge can be used to optimize particle injection.

Keywords computer tomography, diagnostics, DPV-2000, plasma spraying, powder injection, TriplexPro™

1. Introduction

During plasma spraying, the feedstock particles, suspended in a carrier gas, are injected into a plasma gas jet to be melted and accelerated toward the substrate. The injection conditions crucially affect the particle properties and thus the characteristics of the deposited coating.

In most cases, the injection is oriented in radial direction rectangular to the torch axis. Zhang et al. (Ref 1) found experimentally and numerically that at changing carrier gas flows such injector angles close to 90° ensure high particle temperatures and velocities. The radial position of the injector is also an important parameter as the particle dispersion widens considerably if the injector is located more distant from the torch axis (Ref 2). Curved injectors require higher carrier gas flows compared to straight ones (Ref 3).

With increasing carrier gas flow the plasma jet may be deflected downward and its temperature and velocity profiles can become thinner and sharper (Ref 4). However, this seems to be dependent on the prevailing plasma parameters as other results show only negligible cooling and retarding effects (Ref 3), in particular in the jet core (Ref 5). Regarding the viscosity of the plasma gas, Vardelle et al. found that it does not play a major role for particle penetration in the jet whereas plasma jet momentum does (Ref 3).

As feedstock powders exhibit statistically distributed particle sizes and plasma jets show large temperature and velocity gradients at the location of the injection, the particles travel along many different trajectories (Ref 6). Furthermore, plasma fluctuations being distinct for one-cathode torches exert a dispersion effect on particle characteristics (Ref 3, 7). For a given carrier gas flow rate, the particle injection velocity is certainly almost independent on the particle size (Ref 3, 8). However, due to their higher momentum larger particles are found in the lower part of the deposition footprint and may even pass through the plasma plume. In contrast, finer particles can have insufficient momentum and thus bypass the jet. Although being subjected to relatively greater drag forces, large particles accelerate slower due to higher inertia (Ref 9). They exhibit lower temperatures as well because of their larger thermal mass. To achieve a better physical insight into the overall energy and momentum acquired by the particles, the use of volume averaged particle velocities and temperatures is proposed instead of number averaged values. Thus, molten volume

This article is an invited paper selected from presentations at the 2010 International Thermal Spray Conference and has been expanded from the original presentation. It is simultaneously published in *Thermal Spray: Global Solutions for Future Applications, Proceedings of the 2010 International Thermal Spray Conference*, Singapore, May 3-5, 2010, Basil R. Marple, Arvind Agarwal, Margaret M. Hyland, Yuk-Chiu Lau, Chang-Jiu Li, Rogerio S. Lima, and Ghislain Montavon, Ed., ASM International, Materials Park, OH, 2011.

Georg Mauer, Robert Vaßen, and **Detlev Stöver**, Institut für Energieforschung (IEF-1), Forschungszentrum Jülich GmbH, Jülich, Germany; and **Stefan Kirner, José-Luis Marqués, Stephan Zimmermann, Günter Forster,** and **Jochen Schein**, Institut für Plasmatechnik und Mathematik IPM (LPT), Universität der Bundeswehr München, München, Germany. Contact e-mail: g.mauer@fz-juelich.de.

fractions can be determined depending on process conditions (Ref 10).

The carrier gas flow has to be adjusted carefully depending on particle size and density, injector geometry and position, as well as on plasma jet characteristics to achieve optimum heat and momentum transfer. In doing so, the spray pattern centroid position moves vertically (Ref 11). By such optimization, also the variability of coating deposition due to parameter variations can be reduced (Ref 12).

Applying three cathode torches, also the azimuthal position of the injectors can be adjusted to improve particle injection into the non-rotationally symmetric plasma jet. The shapes of such plasma plumes change with the plasma parameters (Ref 13). To identify the optimum setup no simple indicators are available, thus emission computer tomography and in-flight particle diagnostics are applied in this work.

2. Experimental

The experiments were performed by atmospheric plasma spraying in a Multicoat facility (Sulzer Metco, Wohlen, Switzerland). The preliminary injection tests were done with a single-cathode F4 torch at 600 A current and a plasma gas flow of 40 slpm Ar and 10 slpm H_2 (input power 39.4 kW). The powder was an in-house spray dried Al-Mg spinel (d_{10} = 23 µm, d_{50} = 47 µm, and d_{90} = 108 µm) with a feed rate of 4.5 g min^{-1}. The injector internal diameter was 1.8 mm (as far as not denoted differently below). It was aligned vertically with an angle of 90° relative to the horizontal torch axis. The axial position was 6.0 mm from the nozzle exit and the radial distance to the torch axis was also 6.0 mm. The spray distance was 80 mm.

Subsequently, the tomographic investigations were carried out with a three-cathode TriplexPro™ torch (Ref 14) mounted on a six-axis robot. The nozzle diameter was 9 mm; the injector internal diameter was 1.8 mm with an angle of 90° relative to the horizontal torch axis. The azimuthal injector positions are step-adjustable by 20° between 0° and 80°, Fig. 1. The placement of the cathodes inside the gun is indicated as well. For the particle diagnostic measurements the torch was rotated around its axis so that the injector was always aligned vertically. Furthermore, two different injector mounts were applied providing different axial injector positions. Using the ''90° long'' mount, the injector is located 12.5 mm from the nozzle exit, i.e., 8 mm more downstream compared to the ''90° short'' mount. The radial distance of the injector to the torch axis was 12 mm in both cases.

The feedstock was a commercially available 7YSZ HOSP™ powder (Sulzer Metco 204NS, d_{10} = 16 µm, d_{50} = 48 µm, and d_{90} = 88 µm) with a spherical morphology. The feed rate was 20 g min^{-1} and the carrier gas flow was varied. Further spray parameters are listed in Table 1. Case 1 represents a standard parameter, the low power parameters of case 2 are applied for high porous coatings, and case 3 is characterized by high plasma gas flow.

Particle in-flight diagnostics at 200 mm stand-off distance were performed by means of the DPV-2000 system (TECNAR Automation Ltd., St-Bruno, QC, Canada). It enables particle velocities, temperatures, and diameters to be measured. The operating principles are described elsewhere (Ref 15). Temperature measurements are

Table 1 Spray parameters for the TriplexPro™ torch

Case	1	2	3
Current, A	540	470	540
Input electric power, kW	54.6	45.2	60.3
Effective power, kW	30.9	25.3	37.6
Plasma gas, slpm Ar/He	50/4	50/4	75/6

slpm, standard liters per minute

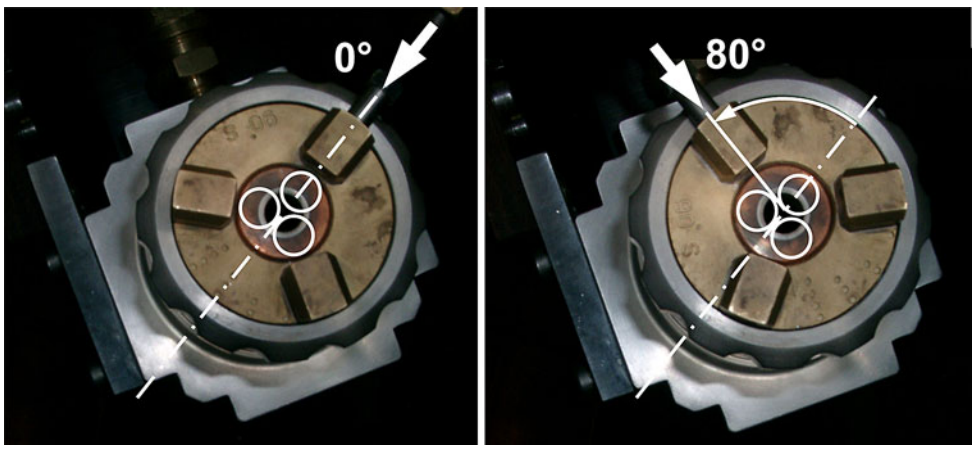

Fig. 1 Azimuthal injector positions of the TriplexPro™ torch being step-adjustable by 20° between 0° and 80°. Circles indicate cathode positions inside the torch

possible between 1000 and 4000 °C, velocity measurements from 5 to 1200 m s^{-1}, and diameter measurements from 10 to 300 μm. The velocity measurement precision is better than ±0.5% but the precision of the absolute temperature and diameter measurements is dependent, in particular on the emissivity characteristics of the particle material. Detailed investigations on this complex subject can be found elsewhere (Ref 16). The measurement results are very self-consistent and the repeatability is found to be better than 1%.

In order to determine the three-dimensional temperature distribution inside the gas jet close to the injector's plane, a computer tomography equipment has been constructed to measure the gas emissivity in visible and near infrared. The tomography setup consists of three CCD cameras mounted at 0°, 90°, and 225°, each one equipped with a different narrow-band interference filter of 10 nm spectral width. By rotating these cameras around the hot gas jet for half a circle, 60 different angles are measured, Fig. 2. This permits to reconstruct a full mapping of the radiation emitted by the jet, assuming that the latter is optically thin and nearly stationary during the measurement time (2-3 min). The Triplex torch, with its fixed electric arc lengths, satisfies this last condition. The tomographically reconstructed image contains 120 cross sections, has a downstream extension of about 40 mm and a resolution of 0.32 mm/pixel. The interference filters have been chosen centered at the main lines of non-ionized Argon (694, 766, and 830 nm). Assuming local thermodynamical equilibrium, the emissivity distribution is converted into a temperature distribution according to a standard calculation based on the Saha equation, whose details are discussed elsewhere (Ref 17).

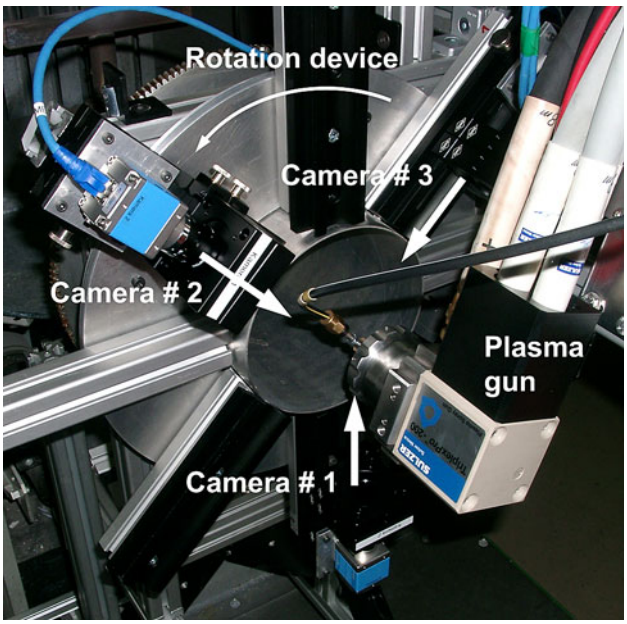

Fig. 2 Computer tomography setup with three CCD cameras with their corresponding interference filters

3. Results and Discussion

3.1 Preliminary Injection Tests Using a Single-Cathode F4 Torch

In-flight particle characteristics were measured by DPV-2000 in spray distance while the carrier gas flow was varied between 2.5 and 5.0 slpm. With increasing carrier gas flow the vertical coordinate (parallel to the injection direction) of the maximum particle flow (not shown) moved down by 3.1 mm. At carrier gas flows below 3.5 slpm, distinctly fewer particles were detected since the injection was obviously not sufficiently deep. The vertical characteristics of the particle velocities were almost identical for the different carrier gas flows, Fig. 3.

The large vertical variation between approximately 250 and 370 m s^{-1} is noticeable. The maximum temperatures varied moderately by approximately 50 K while the overall variation was between 2540 and 2660 °C. With increasing carrier gas flow, the maxima's vertical position moved downward, Fig. 3.

As expected, the larger particles were found in the lower part of the deposition footprint. This is shown in circle diagrams of the particle velocities and temperatures which are plotted against the particle diameters, Fig. 4.

The maximum velocities and temperatures were found commonly for the smaller particles of approximately 45 μm in diameter. The maximum velocities appeared

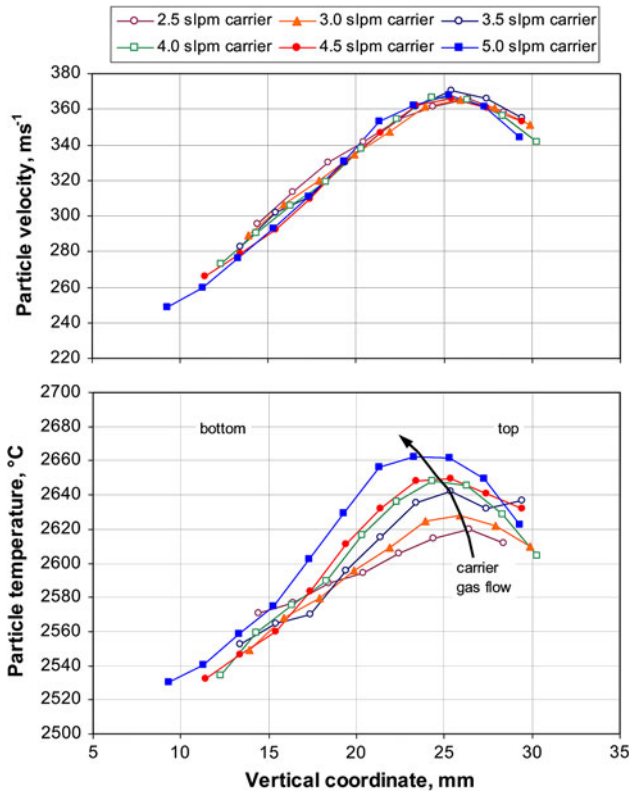

Fig. 3 Vertical characteristics of particle velocities and temperatures at a spray distance of 80 mm (single-cathode F4 torch)

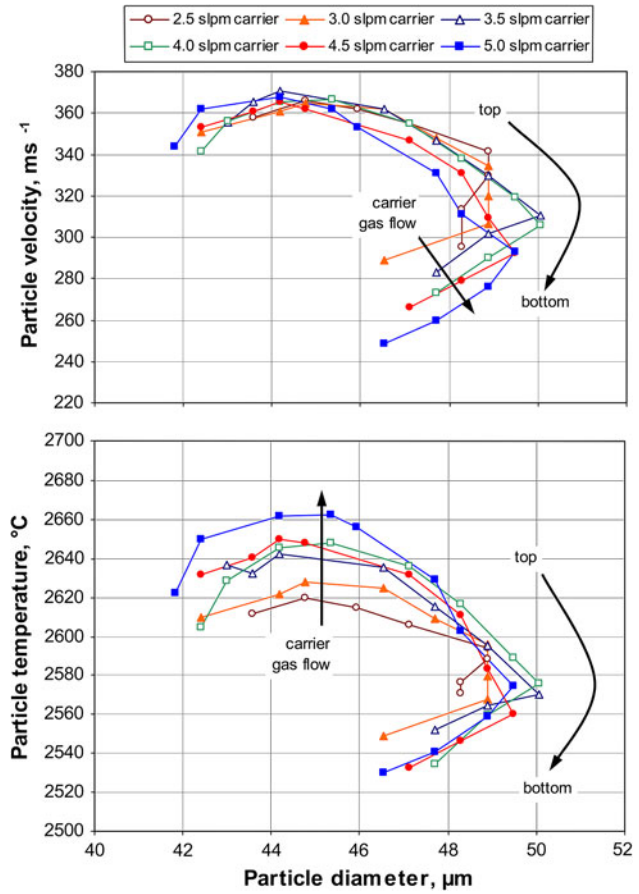

Fig. 4 Circle diagrams of particle velocities and temperatures at a spray distance of 80 mm as a function of particle diameters (single-cathode F4 torch). The lines indicate the vertical course of the measurements from the top to the bottom of the jet's cross section

unaffected by the carrier gas flow, whereas the maximum temperatures increased at raising carrier gas flow. The larger particles above 48 µm showed different behavior. The particles with the lowest trajectories exhibited lower velocities with increasing carrier gas flow while their temperatures were similar.

Obviously, the smaller particles are accelerated efficiently if they are captured by the plume and do not pass through the jet. However, it depends on the injection depth toward the hot plasma core close to the nozzle how efficiently they are heated. In contrast, the larger particles if injected too deep are less accelerated because they pass through the plume. However, they approach the hot core of the jet which provides still appropriate heating.

The experiments with the single-cathode F4 torch showed these further results.

- The variation of the powder feed rate between 2.7 and 6.3 g min^{-1} at constant carrier gas flow 3.5 slpm yielded similar particle characteristics. Only at the highest feed rate slightly decreased particle velocities and temperatures were observed. Hence, for higher powder feed rates the carrier gas flow has to be adjusted.
- The injector diameter was enlarged from 1.8 to 2.0 mm. As a result, the velocities remained almost unaffected while the particle temperatures dropped. The latter could be compensated accurately by increasing the carrier gas flow from 3.5 to 4.3 slpm giving the same carrier gas velocity as before.
- Tapering the end of the injector in the plasma plume's downstream direction had similar effects such as decreased carrier gas flows. Obviously, the radial component of the injection velocity is lower.

3.2 Optical Plasma Diagnostics for the Three-Cathode TriplexPro^{TM} Torch

The three-cathode Triplex plasma torch was initially developed to avoid the strong fluctuating motion of the arc attachment to the anode, without reducing the electric power of a single-cathode torch. The generated gas jet displays a non-rotationally symmetric jet, with a triangular arrangement of three pronounced hot cores outside the torch corresponding to the prolongation of the three cathodic arcs inside the torch. Thus, a so-called ''cage effect'' has been assumed where an optimum particle injection should be easily achieved if the injection direction is between two of these hot cores, which also correspond to regions of higher gas velocity and viscosity and thus of higher viscous drag. This cage effect should be particularly enhanced due to the fact that particles already injected along such injector direction, after reaching the central region of the jet, would meet the third core located opposite to the injector, impeding thus that such particles leave the jet by crossing it. Hence, the relation between injection direction and the triangular structure of high temperature cores inside the jet is a topic worth regarding, which requires a full three-dimensional resolution of the temperature distribution inside the jet like that offered by the computer tomography.

Assuming local thermodynamical equilibrium, the emissivity of the plasma gas is a known function of the gas temperature and therefore, in analogy to the two-color pyrometry, the gas temperature in the jet can be determined from the quotient between two integrated emissivities in very narrow spectral windows. For the typical gas species used with the Triplex torch, these spectral windows correspond to those wavelengths for a maximum emissivity of non-ionized Argon: 689-699 nm, 761-771 nm, and 825-835 nm. Each integrated emissivity contains the radiation emitted by electrons due to transitions between bound atomic states (discrete lines), due to the brake radiation at ions and atoms as well as due to the electron capture by an ion (Ref 17-19). Although the temperature determination at locations near the central region shows an accuracy higher than 500 K, the main deviation source for the temperature reconstruction are the assumption of local thermodynamical equilibrium, with the same temperature for electrons and heavy species, as well as the

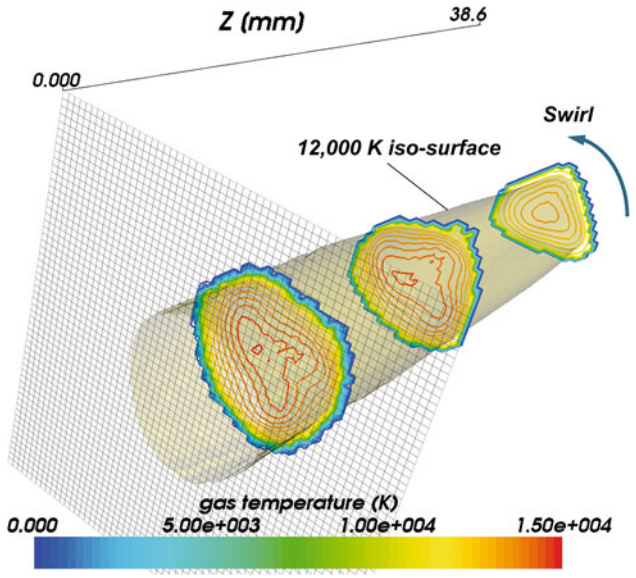

Fig. 5 Tomographic reconstruction of gas temperature distribution (TriplexPro™ torch, case 1, short injector mount), showing the counterclockwise jet rotation; injector plane cross section, two additional downstream sections and surface of 12,000 K. The size of each square tile in the transversal section is 0.3 × 0.3 mm^2

slight modification in the gas composition in downstream direction, with its corresponding change in emissivity.

The presence of the three injectors close to the torch outlet does not allow measuring the tomogram at that location. Nevertheless the use of Helium as a second plasma gas, with its corresponding high viscosity due to the nearly absence of ionization at the typical temperatures outside the torch, ensures a low turbulence level and a reduced radial spreading of the gas jet. Hence, the temperature distribution at the injector's plane can be extrapolated upstream from the results at section located just after the injector planes, by implementing the counterclockwise rotation rate of the gas jet in downstream direction, Fig. 5. This jet rotation is induced by the gas distribution ring inside the torch, in order to improve the interaction between the gas and the electric arcs near to the cathodes.

In addition, the gas velocity distribution can also be estimated at locations close to the torch outlet. Due to the already mentioned high viscosity of Helium, the gas flow at the injectors section can be assumed in a first approximation as nearly laminar. In such case, the viscosity and thermal conductivity are mainly determined by the gas properties and not by the turbulence, and moreover, the nonlinear convective term in the Navier-Stokes equation can be neglected when compared to the diffusion term. Since laminar viscosity and thermal conductivity show a very similar temperature dependence at high temperatures, and since the velocity and temperature stationary equations are similar when neglecting the convective terms, the radial spreading of the laminar flow and thus the resulting radial profile can be assumed to be rather similar for temperature and for the velocity.

Table 2 Plasma jet characteristics determined by tomographic emission measurements (TriplexPro™ torch, cases 1-3, short injector mount)

Case	1	2	3
T_{max}, K	15,000	14,500	16,000
Estimated V_{max}, m/s	1250	1140	1940
Rotation, °/mm	2.63 ± 0.03	3.1 ± 0.2	2.6 ± 0.3

Let $T(r,\theta) = T_{max} f_T(r,\theta)$ represent the temperature distribution at any location denoted by the polar coordinates (r,θ) within the jet at the outlet/injector section, being $f_T(r,\theta)$ the relative profile directly obtained from the tomographic reconstruction of the temperature. The velocity distribution at such section is denoted $V(r,\theta) = V_{max} f_V(r,\theta)$, whereas for the relative distribution profile $f_V(r,\theta) \approx f_T(r,\theta)$ is assumed due to the nearly laminar Argon/Helium flow. By definition, the mass flow $\dot{m}$ and effective power $\dot{W}_{eff}$ are defined by

$$\begin{aligned} \dot{m} &= \int_{section} \rho(T(r,\theta)) V(r,\theta) dr d\theta \\ \dot{W}_{eff} &= \int_{section} \rho(T(r,\theta)) h(T(r,\theta)) V(r,\theta) dr d\theta \end{aligned} \quad \text{(Eq 1)}$$

with $\rho(T)$ and $h(T)$, respectively, the temperature dependent mass and enthalpy density, taken from the calculated tables in Ref 20 for the considered gas mixture. Hence, by taking the plasma gas mass flow $\dot{m}$ and effective torch power $\dot{W}_{eff}$ listed in Table 1, and having determined the relative distribution profiles of temperature and velocity from the tomographic reconstruction, an estimation of the maximum gas velocity (and temperature) is achieved.

The plasma jet characteristics determined by the tomographic reconstruction for the TriplexPro™ torch with the short injector mount are shown in Table 2. The temperatures in cases 2 and 3 were lower due to the lower plasma power and the lower power density, respectively. The gas velocity was mainly affected by the plasma gas flow rate (case 3) and obviously not by the plasma power (cases 1 and 2). The largest downstream velocity in case 3 resulted in the smallest rotation rate of the jet.

The temperature distributions over the jet's cross sections in the plane of particle injection show characteristic non-rotationally symmetric profiles, Fig. 6. The tomographic measurements were carried out without particulate flow into the jet, the positions of the injectors being taken as reference. For the three investigated cases, the orientation of the triangular high temperature region is very similar. Applying the injector position at 40° means that the particles will be injected between two adjacent high temperature cores, which would correspond to an optimal injection according to the cage effect. Unfortunately, for the investigated cases there was no accessible injector position providing injection exactly onto the high temperature core, being the closest position to this condition 0°.

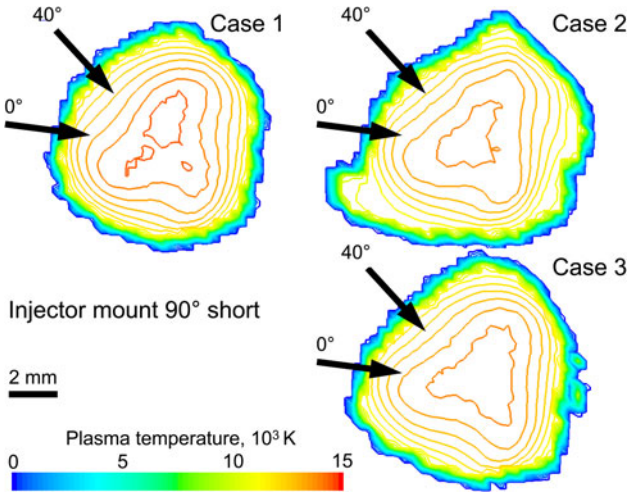

Fig. 6 Tomographic reconstruction of gas temperature distributions (TriplexPro™ torch, cases 1-3, short injector mount) at the injectors section, looking downstream; the arrows indicate the investigated azimuthal injector positions for the particle characterization in section 5

3.3 Particle Characterization at Different Injection Conditions Using a Three-Cathode TriplexPro™ Torch

The DPV-2000 measurements of the in-flight particle properties were carried out in spray distance for the parameter cases 1-3, each with the injector positions providing particle injection between the cores (40°) and close to one core (0°), respectively. For these particle diagnostic measurements the torch was rotated around its axis so that the injector was always aligned vertically. Figure 7 shows the circle diagrams of particle temperatures in spray distance 200 mm as a function of particle diameters for the TriplexPro™ torch and both the injector positions. Here, case 1 (short injector mount) is given as an example. Since the particle velocities exhibit similar developments (not shown), the plasma temperature and velocity distributions seem to have an analogous characteristic which is in contrast to the single-cathode F4 torch (cp. section 3). This may be due to the fact that the cross-sectional areas of the jet are larger and thus the temperature and velocity gradients are smaller.

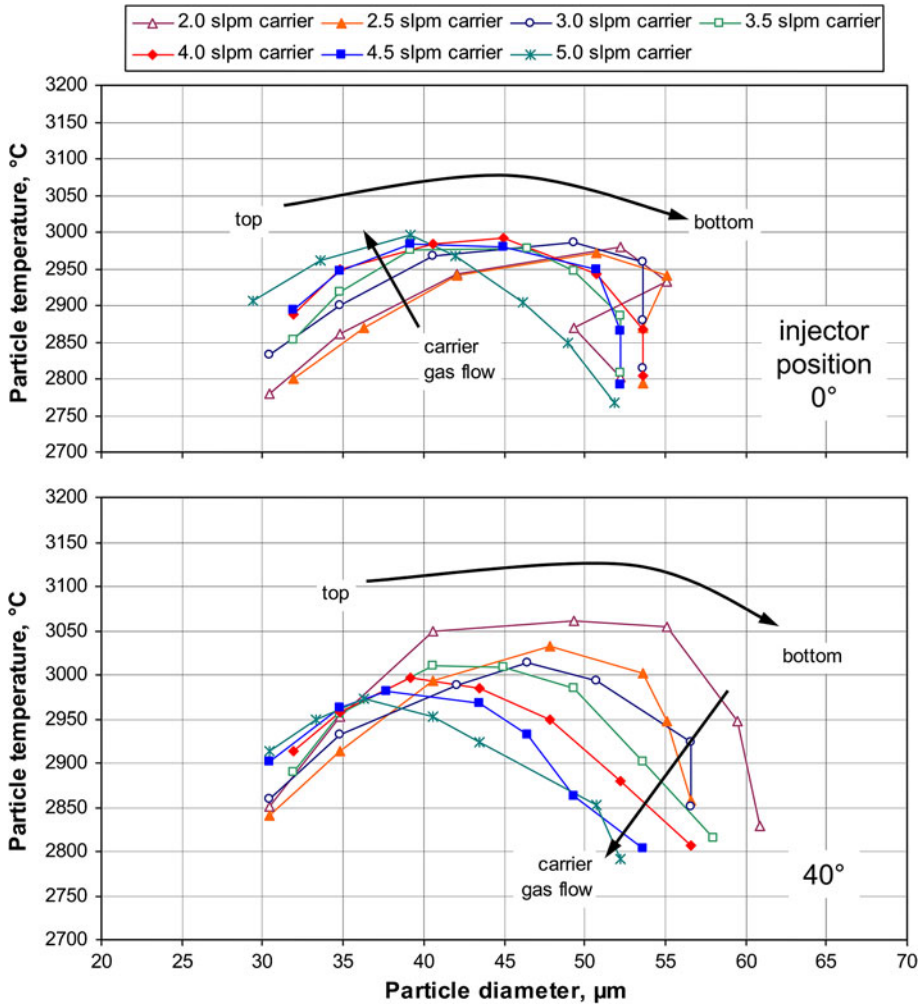

Fig. 7 Circle diagrams of particle temperatures at a spray distance of 200 mm as a function of particle diameters (TriplexPro™ torch, case 1, short injector mount). The arrows indicate the vertical course of the measurements from the top to the bottom of the jet's cross section

Injecting between the high temperature cores at 40°, in particular the larger particles are heated efficiently. Obviously, the core opposite to the injector supports the particles to be kept properly in the jet center. At 0°, however, such blocking core *vis-à-vis* the injector is missing and thus the larger particles easily pass through the hot core of the jet due to their momentum. Hence, their temperature is considerably lower. These findings are completely confirmed by the results for the cases 2 and 3 (not shown).

The coating characteristics are directly affected by the efficiency of the plasma particle interaction. Table 3 shows some coating results for case 1 (short injector mount). Injecting the powder at the 40° azimuthal position between two high temperature cores provides a higher deposition efficiency as well as some lower porosity and surface roughness compared to injection close to one core at 0° position.

The efficiency of the plasma torch operation can be described by the heated particle volume flow. Therefore, the particle temperatures measured over the vertical cross section of the jet (vertical coordinate in Fig. 3) were volume flow averaged

$$\overline{T_p} = \frac{\sum_i T_{p,i} \cdot d_{p,i}^3 \cdot \frac{dn_{p,i}}{dt}}{\sum_i d_{p,i}^3 \cdot \frac{dn_{p,i}}{dt}}, \qquad \text{(Eq 2)}$$

where $T_{p,i}$ is the mean particle temperature, $d_{p,i}$ is the mean particle diameter, and $dn_{p,i}/dt$ is the particle flow rate, each at measurement point i representing a specific vertical coordinate parallel to the injection direction. The results show clearly that in all investigated cases the particle injection between the high temperature cores yields a more efficient particle heating than injecting them close to a core, Fig. 8. In these plots, also the optimum carrier gas flows can be identified for each parameter case. The higher the jet momentum the more distinct the maxima of the particle temperatures are located.

In all three cases, injection between the cores also provides the highest particle velocities (not shown) compared to injection close to a core. However, the differences are relatively small. Thus, particle temperatures are more meaningful when the injection conditions are to be optimized.

Due to the swirl of the plasma jet, the 40° azimuthal injector position does not provide any more an injection exactly between two high temperature cores if the long injector mount is used instead of the short one. In doing so, the injection is moved downstream by 8 mm and thus the temperature profile rotates by approximately 21° (case 1) so that at the 40° position the injection is located closer to one hot temperature core, Fig. 9. Furthermore, it is suggested that in downstream direction the lower viscosity channels between the cores disappear gradually and the high viscosity regions concentrate at the jet center due to

Table 3 Effect of azimuthal injector position on process and coating characteristics (TriplexPro™ torch, case 1, short injector mount)

	Injector position 0° (~onto core)	Injector position 40° (between cores)
Deposition efficiency, %	42.6	48.9
Mercury porosity, %	9.8	9.5
Roughness (R_a/R_z), µm	6.3/36.7	5.6/32.7

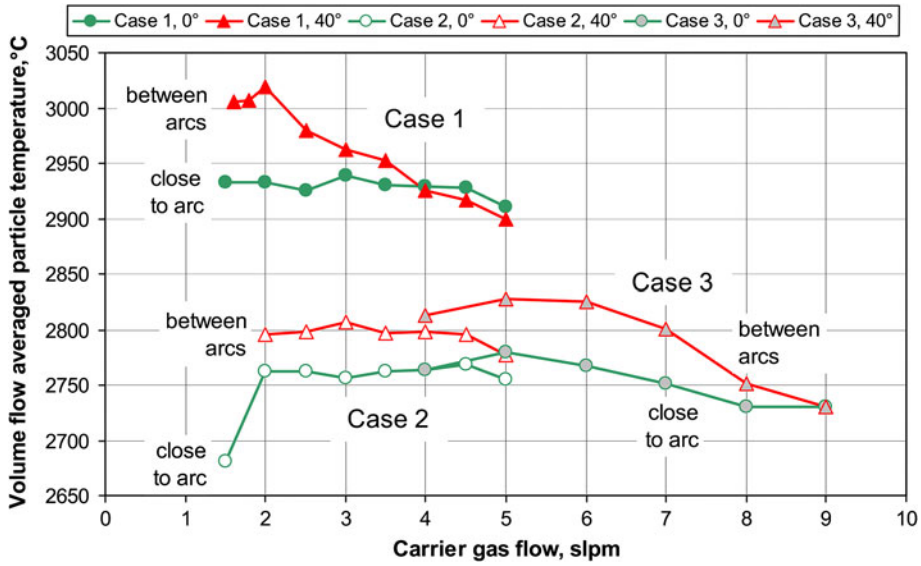

Fig. 8 Volume flow averaged particle temperatures as a function of carrier gas flow and azimuthal injector position (TriplexPro™ torch, cases 1-3, short injector mount)

the radial dissipation of the jet. As a consequence, higher carrier gas flows are necessary to achieve appropriate particle injection. This is indicated by the shift of the maximum volume flow averaged particle temperatures to higher carrier gas flows for all three investigated cases, Fig. 10. It is only natural that the overall particle temperatures are lower if the powder is injected further downstream.

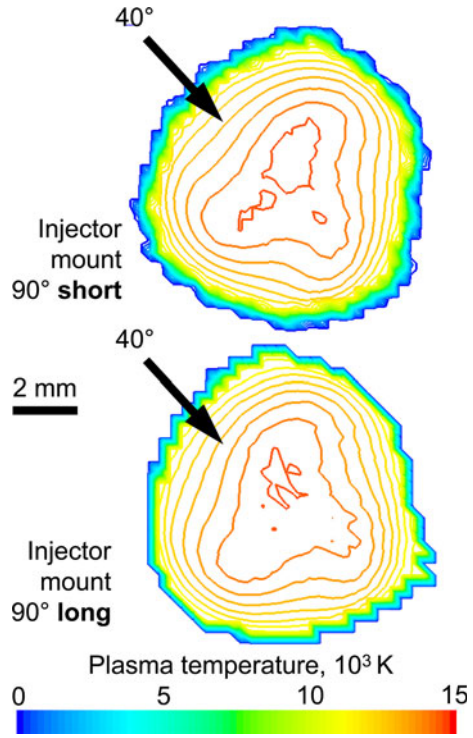

Fig. 9 Tomographic reconstruction of gas temperature distributions (TriplexPro™ torch, case 1, short and long injector mount) at the injectors section, looking downstream; the arrows indicate the investigated azimuthal injector position for the particle characterization

4. Conclusion

The initial injection tests using the single-cathode F4 torch showed that the most important parameter to improve the powder injection is the carrier gas flow. It has to be adjusted carefully to achieve optimum heat and momentum transfer. The particle heating is completed on the very first section of the trajectories close to the nozzle while acceleration happens during longer parts of the flight path. Regarding the particle velocities, the injection must be not too deep to avoid passing through the plume. On the other hand, the highest particle temperatures are achieved if the particles are injected sufficiently deep close to the hot plasma core.

Compared to the single-cathode F4 gun, the TriplexPro™ torch provides jets with larger cross-sectional areas and thus the plasma temperature and velocity gradients are smaller. The tomographic reconstruction of the gas temperature distribution allows to relate the injector direction with the regions of high gas temperature and thus of high gas velocity and viscosity. For all investigated parameter cases with the TriplexPro™ torch the most efficient particle heating corresponds to an injection direction between two high temperature cores, thus confirming the ''cage effect'' which has been assumed theoretically in a multi-electrode torch. Obviously, the core opposite to the injector supports in particular the larger particles to be kept properly in the jet center and prevents them from passing through the plume due to their

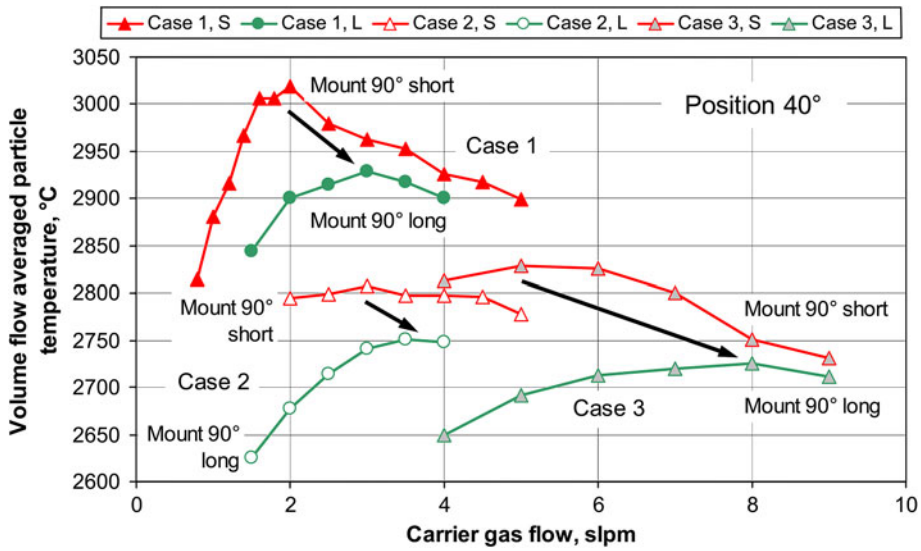

Fig. 10 Volume flow averaged particle temperatures as a function of carrier gas flow and axial injector position (TriplexPro™ torch, cases 1-3, 40° azimuthal injector position). Arrows indicate the shift of the temperature maxima to higher carrier gas flows

momentum. As particle velocities were found to vary only moderately, the particle temperatures are more meaningful when the injection conditions are to be optimized. The results show that particle injection between the hot cores combined with an appropriate carrier gas flow allows the optimization of the achieved process effectiveness as a function of the size of the injected particles.

References

1. W. Zhang, L.L. Zheng, H. Zhang, and S. Sampath, Study of Injection Angle and Carrier Gas Flow Rate Effects in Particles In-Flight Characteristics in Plasma Spray Process: Modeling and Experiments, *Plasma Chem. Plasma Process*, 2007, **27**, p 701-716
2. H.P. Li and X. Chen, Three-Dimensional Modeling of the Turbulent Plasma Jet Impinging Upon a Flat Plate and with Transverse Particle and Carrier-Gas Injection, *Plasma Chem. Plasma Process*, 2002, **22**, p 27-58
3. M. Vardelle, A. Vardelle, P. Fauchais, K.I. Li, B. Dessoubs, and N.J. Themelis, Controlling Particle Injection in Plasma Spraying, *J. Therm. Spray Technol.*, 2000, **10**, p 267-284
4. W. Zhang, V. Srinivasan, L.L. Zheng, and S. Sampath, An Investigation of Particle Injection and Resulting In-flight Particle Behavior During Air Plasma Spraying, *Proceedings of 2006 ASME International Mechanical Engineering Congress and Exposition (IMECE2006)*, Nov. 5-10, 2006 (Chicago, IL)
5. K. Remesh, S.C.M. Yu, H.W. Ng, and C.C. Berndt, Computational Study and Experimental Comparison of the In-Flight Particle Behavior for an External Injection Plasma Spray Process, *J. Therm. Spray Technol.*, 2003, **12**, p 508-522
6. T. Zhang, Y. Bao, D.T. Gawne, B. Liu, and J. Karwattzki, Computer Model to Simulate the Random Behavior of Particles in a Thermal-Spray Jet, *Surf. Coat. Technol.*, 2006, **201**, p 3552-3563
7. E. Meillot and G. Balmigere, Plasma Spray Modeling: Particle Injection in a Time-Fluctuating Plasma Jet, *Surf. Coat. Technol.*, 2008, **202**, p 4465-4469
8. J.R. Fincke, W.D. Swank, and D.C. Haggard, More on the Influence of Injector Geometry and Carrier Gas Flow Rate on Spray Pattern and Particle Temperature, *Thermal Spray: Surface Engineering via Applied Research*, C.C. Berndt Ed., May 8-11, 2000 (Montréal, Québeck, Canada), ASM International, 2000, p 9-14
9. K. Remesh, H.W. Ng, and S.C.M. Yu, Influence of Process Parameters on the Deposition Footprint in Plasma-Spray Coating, *J. Therm. Spray Technol.*, 2003, **12**, p 377-392
10. D. Wroblewski, O. Gosh, A. Lum, D. Willoughby, M. VanHout, K. Hogstrom, S.N. Basu, and M. Gevelber, Modeling and Parametric Analysis of Plasma Spray Particle State Distribution for Deposition Rate Control, *Proceedings of the 2008 ASME International Engineering Congress and Exposition (IMECE2008)*, Oct. 31-Nov. 6, 2008 (Boston, MA)
11. H.B. Xiong, L.L. Zheng, S. Sampath, R.L. Williamson, and J.R. Fincke, Three-Dimensional Simulation of Plasma Spray: Effects of Carrier Gas Flow and Particle Injection on Plasma Jet and Entrained Particle Behavior, *Int. J. Heat Mass Transf.*, 2004, **47**, p 5189-5200
12. V. Srinivasan, A. Vaidya, T. Streibl, M. Friis, and S. Sampath, On the Reproducibility of Air Plasma Spray Process and Control of Particle State, *J. Therm. Spray Technol.*, 2006, **15**, p 739-743
13. J. Schein, K.D. Landes, G. Forster, J. Zierhut, and M. Dzulko, Tomographic Investigation of Plasma Jets Produced by Multi-Electrode Plasma Torches, *J. Therm. Spray Technol.*, 2008, **17**, p 338-343
14. J. Schein, J. Zierhut, M. Dzulko, G. Forster, and K.D. Landes, Improved Plasma Spray Torch Stability Through Multi-Electrode Design, *Contrib. Plasma Phys.*, 2007, **47**, p 498-504
15. G. Mauer, R. Vaßen, and D. Stöver, Comparison and Applications of DPV-2000 and Accuraspray-g3 diagnostic Systems, *J. Therm. Spray Technol.*, 2007, **16**, p 414-424
16. G. Mauer, R. Vaßen, and D. Stöver, Detection of Melting Temperatures and Sources of Errors Using Two-Color Pyrometry During In-flight Measurements of Atmospheric Plasma-Sprayed Particles, *Int. J. Thermophys.*, 2008, **29**, p 764-786
17. J.L. Marqués, G. Forster, and J. Schein, Multi-Electrode Plasma Torches: Motivation for Development and Current State-of-the-Art, *Open Plasma Phys. J.*, 2009, **2**, p 89-98
18. Ya.B. Zeldovich and Yu.P. Raizer, *Physics of Shock Waves and High-Temperature Hydrodynamic Phenomena*, Dover Publ., New York, 2002
19. A.T.M. Wilbers, G.M.W. Kroesen, C.J. Timmermans, and D.C. Schram, The Continuum Emission of an Arc Plasma, *J. Quant. Spectrosc. Radiat. Transf.*, 1991, **45**, p 1-10
20. M. Boulos, P. Fauchais, and E. Pfender, *Thermal Plasmas*, Plenum Press, New York, 1994